Observasjon validering, modellering – historiske linjer og nye resultater i norsk forskning om jordens tyngdefelt[1]

Christian Gerlach, Michal Šprlák, Katrin Bentel and Bjørn R. Pettersen

Vitenskapelig bedømt (refereed) artikkel

Christian Gerlach et. al: Observation, validation, modeling – historical lines and recent results in Norwegian gravity field research

KART OG PLAN, Vol. 73, pp. 128–150, POB 5003, NO-1432 Ås, ISSN 0047-3278

The history of modern gravity field research stretches back to the second half of the 19th century, when international cooperation was established through the foundation of the *Mitteleuropäische Gradmessung*, the predecessor of today's International Association of Geodesy (IAG). Norway was among the first nations collaborating in this international endeavor and is thus one of the oldest member states of IAG. Gravity field activities in Norway were in many cases inspired by and connected to the activities and resolutions of IAG, e.g., the establishment of the European gravimeter calibration baseline in the 1950s. This also holds for some of the recent gravity field related projects on which we report in this paper. They are carried out at the Norwegian University of Environmental and Life Sciences in Ås (UMB), formerly the Agricultural University of Norway (NLH). Olav Mathisen, to whom we dedicate this contribution on the occasion of his 80th birthday in 2012, was engaged in gravity field research over the past decades, first as an observer and geodesist at the Geographical Survey of Norway (now called *Kartverket*) and later as professor of surveying at NLH. We use this occasion to put the current research activities into a historical perspective. We present new validation results of the gravity gradiometry satellite mission GOCE by comparison with deflections of the vertical in Norway (many of which Olav Mathisen had observed) and discuss mathematical techniques for regional gravity field representation with radial basis functions as an alternative to classical approaches.

Keywords: gravimetry, deflections of the vertical, GOCE, gravity field modeling, radial basis functions

Christian Gerlach, prof. II, dr. Commission for Geodesy and Glaciology, Bavarian Academy of Sciences and Humanities, Alfons-Goppel-Str. 11, 80539 München. E-mail: Gerlach@keg.badw.de

Michal Šprlák,[2] *Katrin Bentel and Bjørn R. Pettersen*. Department of mathematical sciences and technology, Drøbakveien 31, NO-1432 Ås.

Historical remarks

The theoretical foundations for gravimetric measurements and gravity field modeling were developed in the 17th and 18th century and are connected to the works of, among others, Galilei, Huygens, Newton, Bouguer, Clairaut, Laplace, Legendre and Poisson. Gravimetric studies at that time were used to determine the value of the gravitational constant, the mean density and mass of the Earth as well as its flattening. Until 1830, gravimetric observation methods were based on the oscillation periods of pendulums. Gravimetric surveys were carried out with transportable field equipment (see, e.g., Torge, 1989). Both absolute and relative pendulums were constructed, the latter only providing gravity differences with respect to an absolute reference point. The first determinations of gravity in Norway were made by Edward Sabine at two stations in Hammerfest and Trondheim in 1823 (Hansteen, 1825). Around that time, Sabine also recognized the possibility to estimate the mass

1. Denne artikkelen er skrevet til Festskrift Olav Mathisen. Alle artiklene fikk ikke plass i festskriftet (nr. 1, 2013) og denne artikkelen måtte vente. Vi trykker den her som en fortsettelse av festskriftet.
2. New address from 2013: Department of Mathematics, Faculty of Applied Science, University of West Bohemia, Univerzitní 22, 306 14 Plzeň, Czech Republic

distribution of the upper layer of the Earth by means of gravity measurements (Sabine, 1825; see also Torge, 1989). The accuracy of gravity observations at that time was in the range of 5–10 mGal or worse.

It was, however, not before the 1860s, when intense scientific research on the gravity field began. Before that time, geodetic surveys had been carried out by several countries as basis for topographic maps or in order to study the general shape of the Earth, i.e. the flattening of the ellipsoid. In Norway, astronomical measurements had been carried out since 1780 for the purpose of positioning and orientation of trigonometric networks (Pettersen 2009). Later, measurements were carried out by Christopher Hansteen in 1816/17 and 1847 to determine the longitude difference between Oslo, Stockholm and Copenhagen (see Jelstrup, 1929; Pettersen 2002, 2006). A significant intensification of scientific research on the gravity field of the Earth started in the 1860ies. Johann Jakob Baeyer, officer of the Prussian General Staff and director of the Geodetic Institute in Berlin, proposed to the Prussian King in 1861 to establish an official cooperation between central European states to study the shape of the Earth. He proposed to investigate various effects which never before had been taken care of in geodetic meridian arc measurements or topographic surveys, namely the precise determination of the curvature of the figure of the Earth and its scientific implications, e.g., its dependency on topography. In Baeyer's terminology the figure of the Earth is the mathematical figure as defined by Gauss (1828), i.e. an equipotential surface at mean sea level, later called the *geoid* by Listing (1873). The king accepted Baeyer's proposal for a *Mitteleuropäische Gradmessung* and ordered the Prussian Ministry of Foreign Affairs to invite the central European states to participate. By 1862, 15 states had expressed their willingness to cooperate. Norway was one of them. Dedicated national commissions were founded to carry out the work. In 1864 the representatives of the participating countries met in Berlin for the first international geodetic conference. They agreed to perform trigonometric and astronomical observations as well as precision leveling. Referring thereby each of the national leveling networks to mean sea level forms the basis for comparing heights throughout Europe. Determination of the curvature of the Earth was based on astronomical observations, from which deflections of the vertical are derived as the difference between the astronomical and the ellipsoidal coordinates. In Norway, astronomical observations were carried out between 1865 and 1894 by astronomy professors Carl Fredrik Fearnley and Hans Geelmuyden. A geodetic meridian arc was connected to the Swedish arc in the south and was extended to Levanger north of Trondheim. Accurate baselines were established at each end (Pettersen 2007). Astronomical activities were then interrupted until the 1920ies when H. Henie carried out astronomical observations in Spitzbergen and H.J. Jelstrup began expanding the net of Laplace stations in mainland Norway.

The aims of the *Mitteleuropäische Gradmessung*, although formulated in 1864, are still on the agenda today. Of course the methodologies have changed. National triangulation networks have been replaced by global navigation satellite systems (GNSS). Deflections of the vertical are only observed in special applications because in most cases the huge amount of terrestrial gravity data makes them obsolete for modeling the fine structures of the geoid. The scientific objectives, however, are still valid today. One of the objectives of ESA's satellite mission GOCE (ESA, 1999) is to support global unification of height systems, a task very similar to the 1864 idea of comparing the national height systems throughout Europe. At the time of Baeyer, deflections of the vertical were required to reduce trigonometrically observed zenith distances for determination of precise trigonometric heights. Geoid heights were required for reduction of measured arc lengths down to the surface of the ellipsoid. Today, geoid heights – besides their use in geophysical applications – are used for transformation between ellipsoidal heights as derived from GNSS and heights of the national leveling networks, e.g. orthometric heights. Recently, Canada and U.S.A. have decided to completely abolish leveling networks for the realization of their vertical reference frames.

Instead, a precise geoid model will define the vertical datum. It can be foreseen that this approach will be followed by many more countries in the future.

Getting back to the time after the 1864 Berlin conference, the *Mitteleuropäische Gradmessung* gave rise to an advent in gravimetric research. In 1887 Robert Daublebsky von Sterneck, staff of the Austro-Hungarian military, developed a relative pendulum apparatus for field measurements with an accuracy of 5 mGal and observation times of about 1 day per station. It was used in many countries and by 1912 already 2500 gravity values were observed. In 1892 a set of Sterneck pendulums were purchased by the Norwegian commission. One of these instruments accompanied Fridtjof Nansen on his Fram expedition to the polar seas (1893–96). The ship froze in for three years and drifted with the ocean currents. It served as an observatory of several phenomena and obtained the first gravity observations at sea. The other instrument was used at 6 stations in northern Norway in 1893 and at 8 stations in southern Norway in 1894 by physics professor O.E. Schiøtz (1894, 1895). He used the University Observatory in Oslo as his reference site and listed his results with 5 decimals. The results fit well to those obtained by Nansen at the reference point in Oslo prior to his expedition. In his 1895 report Schiøtz also computed gravity anomalies and correlated them to geological features. The instrument used by Schiøtz was still in use when G. Jelstrup of the Geographical Survey of Norway (NGO) connected a new reference point in the Geological Museum in Oslo to the reference point in Potsdam, Germany. With the advent of relative gravimeters it became more and more important to realize a precise absolute gravity base to which the relative values could be linked. The old Potsdam System of 1909 was established to provide a global reference point based on the measurements carried out by Kühnen and Furtwängler between 1898 and 1904 (Kühnen and Furtwängler, 1906).

International geodetic research collaborations were ended by World War I and only a few neutral states tried to keep the organization alive – Norway among them. In 1919 geodetic research collaboration was reorganized as a section of the newly established International Union of Geodesy and Geophysics (IUGG). Later this section became the International Association of Geodesy (IAG) with its thematic commissions[3]. At the 1922 IUGG General Assembly in Rome the need for many more gravity measurements was expressed to allow geoid determination based on the equation developed by George Gabriel Stokes in 1849 (see equation (5)). At the same time, isostatic theories were established and Vening-Meinesz developed his seagravimeter for applications in submarines. In addition, the first static relative gravimeters were developed. They allowed higher precision and a much shorter observation time per station. Instruments by LaCoste and Romberg were built since 1939 and those by Worden by 1948. In 1946 G. Nörgaard of the Danish Geodetic Institute measured the gravity difference between Oslo and Copenhagen with two Nörgaard gravimeters (Trovaag and Jelstrup, 1950; see Figure 1). In 1948 NGO purchased Nörgaard gravimeter number 382 for a thorough survey of Norway. From 1948–1949 several gravity connections were measured between Oslo and other capitals. In the sequel gravity was measured along the lines of the first order leveling network. Later NGO acquired additional relative gravimeters by Worden in 1953 and by LaCoste and Romberg in 1969. At the 1951 IUGG assembly recommendations were given for the establishment of gravimeter calibration lines. Following these recommendations, the Department of Geodesy and Geophysics at the University of Cambridge made its pendulum apparatus available, and Norway established a calibration line from Hammerfest via Tromsø, Bodø, Trondheim and Oslo to Bad Harzburg, Germany. At the 1954 IUGG assembly it was decided to establish a European calibration base by extending the Norwegian line via Munich to Rome.

By 1956 the Norwegian section of the line contained 102 points. About 3600 gravity measurements had been conducted along leveling lines. By 1962 the gravity net contained

3. In IAG's current structure Commission 2 deals with the gravity field. For a list of sections and commissions established since 1948 see Drewes, 2012.

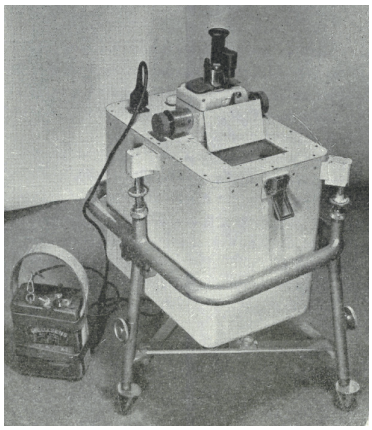

Figure 1: Nörgaard-Gravimeter from Elektrisk Malmletning A/B, Stockholm [source: Trovaag and Jelstrup, 1950].

5200 stations, many with multiple observations. The reference station was at the Geological Museum in Oslo, which was tied to several other reference stations in Denmark, England, Finland, Germany, Iceland, Sweden, and USA (Sømod, 1957). One of the most remarkable ties is probably the one to Anchorage, Alaska, which was performed on SAS's inaugural flight on the North Pole air-route. However, until the end of the 1960ies there had been no attempts to compute a Norwegian geoid model from the available gravity data. Later it was Olav Mathisen who had used existing deflections of the vertical to determine a first regional geoid model over Norway. Today regional geoid models are based on gravity values rather than deflections of the vertical, because much more gravity observations are available (in Norway more than 70.000 gravity stations compared to approximately 120 astronomical stations). However, deflection data is very useful for validation purposes as will be shown below.

When LaCoste & Romberg gravimeters were introduced in Norway, the gravimetric net was reobserved and extended during the 1970s. This forms the core of the national gravity database. Olav Mathisen was the last observer in Norway to use the Nörgaard gravimeter, and the first one to use a LaCoste & Romberg (Bjørn Geirr Harsson 2012, private communication). Absolute gravimetry was re-introduced to Norway in the 1990s when free fall instruments visited from abroad. Since 2004, the Norwegian University of Environmental and Life Sciences at Ås has conducted its own observing program with its state-of-the-art free-fall absolute gravimeter FG5 number 226. This has led to a new database of very accurate absolute stations (Breili et al., 2010). Time series of absolute gravimetry at selected stations allow derivation of current epoch reference values. Recomputation of the national gravity net to current epoch is used to validate results from the GOCE satellite (Šprlák et al., 2012).

Observation, validation and modeling of the Earth's gravity field

Gravity field modeling can be performed on global or regional scales. The two approaches differ in application, resolution, input data and mathematical modeling. Global modeling deals with the deviations of the true gravity field from the gravity field of a mean Earth ellipsoid at resolutions of typically 10 to 50 km. Regional modeling cares for the deviations of the fine structures of the geoid from such a global model. Therefore, global and regional modeling cannot be seen as independent of each other, but global models provide the background for regional refinements. Basis for all global gravity field models is the observation of the mean global field from satellites. In the beginning of the satellite era, satellite positions were observed by cameras and satellite laser ranging from the ground. Deviations between the observed orbit and a nominal orbit computed from a priori knowledge were used to improve global gravity field models. Today, there are dedicated satellite gravity missions of which the U.S.-German Gravity and Climate Experiment GRACE (Tapley et al., 2004) and ESA's Gravity and Steady-State Ocean Circulation Explorer GOCE (ESA, 1999) are the most important. The two missions are complimentary. GRACE observes the global structures of the gravity field with very high precision. This allows detection of tiny temporal variations, caused, e.g., by seasonal variations in ground water or by melting of the large ice sheets in Greenland and Antarctica. However, the spatial resolution is limited to

a few hundred kilometers for monthly gravity field models and about 200 km for their longterm average. GOCE is designed to observe finer structures of the gravity field down to spatial resolutions of about 80–100 km. Modelers try to combine such satellite data with terrestrial data in an optimal way with respect to the error budget of the available data. Therefore it is worthwhile to investigate the optimal mathematical parameterization of the regional field as well as to test the quality of the data by mutual comparisons and to investigate possible systematic deviations. Thus, application of the new type of satellite observations requires selection of a proper mathematical formulation as well as data validation. At the 2011 IUGG assembly, IAG established a joint study group (JSG0.3) to investigate different methodologies in regional gravity field modeling as well as a joint working group (JWG2.3) for the assessment of GOCE geopotential models. The authors of the current paper are engaged in both of these groups and basic ideas as well as current results of their work are reported in the subsequent sections.

GOCE validation with astronomical observations in Norway

General concept of validation

The objective of GOCE to determine the global gravity field to the level of 1–2 cm in terms of geoid heights and 1 mGal in terms of gravity for spatial scales of 100 km or less, is extremely demanding. In order to ensure the quality of the GOCE products, ESA has set up a complex data processing strategy consisting of data preprocessing, internal and external calibration of the observations and the estimation of global gravity field models (GGFM). These models are provided as sets of spherical harmonic coefficients $\{\bar{C}_{lm}, \bar{S}_{lm}\}$ of degree and order (d/o) l and m, which allow computation of the gravitational potential (or any other gravity field functional) according to

$$V(P) = \frac{GM}{R}\sum_{l=0}^{L}\left(\frac{R}{r_P}\right)^{l+1}\sum_{m=0}^{l}\left(\bar{C}_{lm}\cos m\lambda_P + \bar{S}_{lm}\sin m\lambda_P\right)\bar{P}_{lm}(\cos\theta_P). \quad (1)$$

The maximum degree L is connected to the spatial resolution Δ (half wavelength) by the following rule of thumb

$$\Delta = \frac{20000\,\mathrm{km}}{L}. \quad (2)$$

The GGFMs are produced by the High-level Processing Facility (HPF) comprising a consortium of 10 European university and research institutions (Rummel et al., 2004). They follow three competitive strategies for data filtering and analysis (Pail et al., 2011). We may thus expect differences between the different solutions. In view of the demanding quality requirements and the different processing strategies, validation of the GGFMs is a crucial task. It is performed by comparison with independent data (Koop et al., 2001) which allows verification of the entire data processing chain (observation, calibration, analysis).

In the present paper we present validation results of the GOCE GGFMs provided by ESA through HPF by comparison with deflections of the vertical in Norway. Basically, this corresponds to a validation of the inclination of GOCE geoid models in north-south and east-west directions. Similar comparisons have been performed by Voigt et al. (2010) and Voigt and Denker (2011) using deflections of the vertical in Germany and by Hirt et al. (2011) using deflection data in Europe and Australia. Of course also other types of terrestrial data have been employed for validation, e.g. gravity values (see e.g. Šprlák et al., 2012), regional or global geoid models (see e.g., Šprlák et al., 2011; Janák and Pitoňák, 2011) and point values of geoid heights derived from GPS/leveling (see, e.g., Gruber et al., 2011; Guimarãeas et al., 2012). The results of these studies depend on the quality of the terrestrial data, the quality of the GGFMs, the study region and the spectral behavior of the functional under consideration. In essence they all have proven that the representations of the Earth's gravity

field by the three different analysis strategies of HPF are reasonably consistent and that the entire processing chain is of high quality.

GOCE global gravity field models

ESA provides GGFMs based on three different analysis strategies. These are (Rummel et al., 2004)

– the *direct approach*, coordinated by the French space centre, CNES, Toulouse
– the *time-wise approach*, coordinated by the Institute of Navigation and Satellite Geodesy of the Technical University Graz, Austria and
– the *space-wise approach*, coordinated by the section of Surveying, Geodesy and Geomatics of the Polytechnic University of Milan, Italy.

The *direct approach* is based on orbit perturbation theory. It uses a priori satellite orbits, an a priori gravity field model, GPS observations of the GOCE satellite and the gravitational gradients measured by GOCE to set up normal equations for gravity field determination in an iterative manner. The *time-wise approach* uses GPS-based gravity potential values and GOCE gradients as time-series of observations in a least-squares solution; it does not employ any a priori information on the gravity field. The *space-wise approach* considers the spatial correlations between the observations and employs a collocation approach to retrieve the gravity field coefficients. GGFMs based on these approaches have first been provided by Bruinsma et al. (2010) for the direct method, Migliaccio et al. (2010) for the space-wise approach and Pail et al. (2010) for the time-wise method. These models were based on only two months of GOCE observations and officially are provided as GOCE release 1. In the meanwhile release 2 (based on 8 months of data) and release 3 models (based on 15 months) are available. In addition, there exist combinations of the three releases of time-wise models with the best currently available GRACE model ITG-GRACE2010s, provided by the Institute of Theoretical Geodesy of the University Bonn, Germany (http://www.igg.uni-bonn.de/apmg/index.php?id=itg-grace2010). These combined models are labeled GOCO (Gravity Observation Combination) and the latest issue is GOCO03s (Mayer-Gürr et al., 2012). GOCO models are produced by the GOCO consortium, which is composed of institutes of the Technische Universität München, Graz University of Technology, the Universities of Bonn and Bern and the Austrian Academy of Sciences (see www.goco.eu). In order to provide further information on the general improvement brought by the new type of satellite gravity data we also compare the terrestrial data to the model EGM96 (Lemoine et al., 1998) which was the state-of-the-art GGFM before the era of GRACE and GOCE. It is also the only model in our study which represents a combination of satellite data (at that time mainly satellite-laser tracking) and terrestrial data in the form of 0.5° x 0.5° block mean values of surface gravity anomalies. All other GGFMs are purely based on satellite data.

Deflections of the vertical in Norway

For the purpose of GOCE validation, various sets of independent terrestrial data are available in Norway. Comparisons with a regional geoid model and surface gravity data (block mean values as well as point values) have already been performed (Šprlák et al., 2011 and Šprlák et al., 2012). Here we extend these comparisons to deflections of the vertical at more than 100 observing stations. The astronomical coordinates of these stations have been observed in the time span of several decades with various astronomical instruments and with inhomogeneous accuracy. Astronomical positioning was obtained in ten Laplace stations with a Prin transit instrument between 1923 and 1928 (Jelstrup, 1929) by the Geographical Survey of Norway for the purpose of orienting the geodetic first order network. Further extensions were made with an Askania transit instrument between 1930 and 1950. A Wild T4 was used to establish 27 Laplace stations between 1958 and 1969. Olav Mathisen was the most productive observer. He also identified the technical origin of a systematic error with T4-observations and suggested to the manufacturer that certain changes be

made to the instrument (Björn Geirr Harsson, 2012, private communication). Further observations of vertical deflections were made during the 1970s with Wild T2 and Zeiss Ni 20 instruments (Blankenburgh, 1987). A total of 96 stations resulted from five decades of efforts. Some were reobserved as new instruments were introduced. Vertical deflections were determined for further 22 stations in 1981 and 1985 with a zenith camera (Danielsen and Sundsby, 1995) leading to a database of 118 stations in total. Table 1 shows the mean standard deviations obtained with each instrument type. The magnitude of the deflections of the vertical is in the order of ±20“ with a mean variation of about 5“. Figure 2 shows the geographical distribution of the observing stations as well as the deflections (indicated by arrows) against the background of the EGM2008 quasi-geoid. EGM2008 is a combined global model (satellite and terrestrial data) of ultra-high maximum spherical harmonic degree.

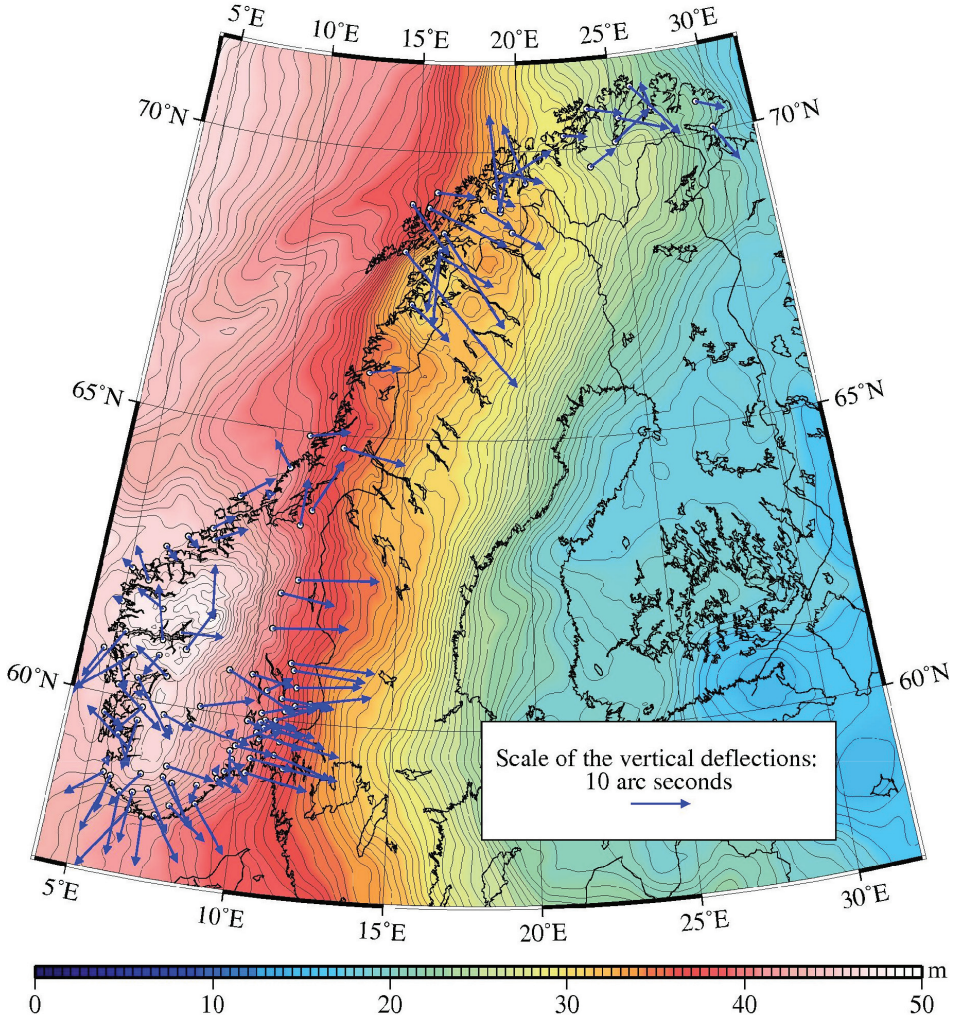

Figure 2: The total deflection of the vertical at 118 stations in Norway against the background of the EGM2008 quasi-geoid model.

Table 1: Mean standard deviations for different types of astronomical instruments for the south-north (ξ) and west-east (η) components of the deflection of the vertical.

	Transit instrument	T4	T2	Zenith camera
Std.dev. (ξ)	0.18“	0.23“	0.44“	0.15“
Std.dev. (η)	0.24“	0.08“	0.44“	0.18“

L=2190, corresponding to a resolution of about 10 km (Pavlis et al., 2012). The astronomical observations are unevenly distributed over Norway. The majority of points are located along the coast of southern Norway. After identifying and removing eight outliers from the database of deflections, the remaining 110 stations were used in the following analysis.

Validation methodology

The north-south (NS) and west-east (WE) component of the deflections of the vertical can be computed from a GGFM according to

$$\xi_{GGFM}(P) = -\sum_{l=0}^{L}\sum_{m=0}^{l}\left(\Delta\bar{C}_{lm}\cos m\lambda_P + \Delta\bar{S}_{lm}\sin m\lambda_P\right)\frac{\partial\bar{P}_{lm}(\sin\varphi_P)}{\partial\varphi}$$
$$\eta_{GGFM}(P) = -\frac{1}{\cos\varphi_P}\sum_{l=0}^{L}\sum_{m=0}^{l} m\left(\Delta\bar{S}_{lm}\cos m\lambda_P - \Delta\bar{C}_{lm}\sin m\lambda_P\right)\bar{P}_{lm}(\sin\varphi_P). \quad (3)$$

Evaluation of these equations using the spherical coordinates of the observing stations allows mutual comparison with the observed deflections. The latter are derived by comparing the ellipsoidal coordinates (φ,λ) of the station with the astronomical ones (Γ,Λ)

$$\begin{aligned}\xi_{astro}(P) &= \Phi_P - \varphi_P \\ \eta_{astro}(P) &= \left(\Lambda_P - \lambda_P\right)\cos\varphi_P.\end{aligned} \quad (4)$$

Two aspects are important for the comparison:

– *Definition of the vertical deflections*. Observed deflections are defined as the difference between astronomical and ellipsoidal coordinates. This definition is referred to as Helmert's definition (Jekeli, 1999) with geometrical meaning (the physical plumb line is related to the ellipsoidal normal). In contrast, deflections derived from a GGFM have a gravimetric meaning (the ellipsoidal normal is replaced by the direction of the normal gravity vector). Reductions need to be applied to relate the two definitions.
– *Spectral content of the vertical deflections*. Observed deflections contain all frequencies of the Earth's gravity field up to infinity. Their modeled counterpart, however, is restricted to the maximum d/o of the employed GGFM. In order to make the spectral content consistent, either the observations need to be filtered or the missing high frequencies of the modeled deflections need to be reconstructed from additional data. We follow the second option, which is known as the spectral enhancement method (SEM) and is explained later.

Following Jekeli (1999), several reductions need to be applied to the modeled deflections to make them comparable to the observed deflections. These are, assuming that the modeling is based on standard harmonic expansions in spherical approximation on the surface of the telluroid in the tide-free system:

– ellipsoidal reduction $\delta\xi^{\text{ell}}$ because the modeled deflections are based on spherical approximation and thus are oriented along the geocentric radius vector rather than along the ellipsoidal normal,
– permanent tidal reduction $\delta\xi^{\text{tide}}$ to take care of the fact that the observed deflections are given in the mean permanent tidal system, while the modeled coefficients

are given in the tidal system defined by the employed GGFM (often this is the tide-free system)
- topographic reduction $\delta\xi^{topo}$ if the synthesis is performed on the telluroid rather than on the Earth surface,
- reduction $\delta\xi^{curv}$ for the curvature of the normal plumb line which links the direction of the normal gravity vector (gravimetric definition) to the direction of the ellipsoidal normal (geometric definition) and
- reduction $\delta\xi^{g}$ which stems from approximating, in the definition of the gravimetric deflections, actual gravity by normal gravity.

Equations for these reductions can be found in Jekeli (1999). Because the database of observed deflections, originally referring to the European Datum ED50, had been transformed to WGS84 by *Kartverket*, additional reductions for datum origin and orientation effects did not have to be considered. In addition to the reductions given in the literature, we also evaluated a

- reduction $\delta\xi^{pgr}$ due to postglacial rebound. This might be relevant in areas of pronounced rebound signals like Fennoscandia, if the terrestrial deflections were observed many decades prior to the reference epoch of the GGFM.

Since the ellipsoid of revolution does not show any dependency on longitude, several of the above reductions do only apply to the NS-, but not to the WE-component. For the latter, only the reductions $\delta\eta^{topo}$, $\delta\eta^{g}$ and $\delta\eta^{pgr}$ remain. The reduction due to postglacial rebound has been obtained by numerical differentiation of the land uplift model NKG2005LU (Ågren and Svensson, 2007).

We have analyzed the magnitudes of the reductions at the 118 astronomical stations and found $\delta\xi^{pgr}$ to be the largest reduction. If evaluated over a period of one century the effect is of the order of a few tenths of an arc second. The other reductions are smaller, some by several orders of magnitude. The statistics of the reductions are given in Table 2. Relating the magnitude of the reductions to the accuracy of the observed deflections, which is in the order of a few tenths of an arc second (see Table 1), we find that the reductions $\delta\xi^{tide}$, $\delta\xi^{g}$ and $\delta\eta^{g}$ are negligible. For the observations in our database the reduction due to postglacial rebound is smaller than the values in Table 2, because the observations were made less than one century ago. However, a lack of information of the exact year of observation for several of the stations in the database did not allow a consistent reduction of the postglacial rebound effect. Therefore we decided not to apply it. We estimate that neglecting the postglacial rebound reduction affects our modeling results by about 0.1" – 0.2".

Table 2: Statistics of data reductions for 118 astronomical stations in Norway ($\delta\xi^{pgr}$ and $\delta\eta^{pgr}$ are given in ´´/century).

Reduction	min. [´´]	max. [´´]	mean [´´]	std. dev. [´´]
$\delta\xi^{ell}$	–0.08	0.04	–0.02	–0.02
$\delta\xi^{tide}$	–0.007	0.011	0.010	0.001
$\delta\xi^{topo}$	–0.11	0.04	0.00	0.02
$\delta\xi^{curv}$	0.00	0.36	0.07	0.07
$\delta\xi^{g}$	–0.0004	0.0014	0.0000	0.0002
$\delta\xi^{pgr}$	–0.45	0.25	–0.01	0.21
$\delta\eta^{topo}$	–0.09	0.06	0.00	0.02
$\delta\eta^{g}$	–0.0004	0.0006	0.0001	0.0002
$\delta\eta^{pgr}$	–0.04	0.47	0.23	0.10

After application of all relevant reductions, the comparison between observed and modeled deflections still suffers from spectral inconsistencies. The resolution of the modeled deflections is limited by the maximum degree L of the GGFM. Thus they represent only a smoothed version of the terrestrial observations and a considerable part of the differences between the two sets of data is due to omitting the short-scale signal structures in the modeled deflection. The magnitude of this omission error can be quantified on global average from a degree variance model. Blending degree variances of EGM2008 with the terrain reduced model of Flury (2005) for

the ultra-high degrees, we find an omission error of about 3" above the resolution of GOCE GGFMs, which is not negligible (omission errors in rough terrain will be even larger than this global average). In order to overcome the spectral inconsistency we try to reconstruct the omitted signal by the spectral enhancement method (SEM). The principle is depicted in Figure 3. Thereby the spectrum is separated into three degree bands, the low to medium degrees, the high degrees and the ultra-high degrees. The low to medium degrees are computed from the GGFM under investigation. In our case this is one of the GOCE-based GGFMs. The high degrees above the resolution of GOCE are reconstructed from EGM2008. The ultra-high degrees above the resolution of EGM2008, i.e. above d/o 2190, still amount to an omission error in the order of 0.4" on global average. Because these short scale structures of the gravity field are strongly correlated to the topographic masses, they can be modeled to a large extent from a digital elevation model (DEM). Therefore a residual terrain model (RTM; Forsberg, 1984) is formed as the difference between an ultra-high resolution DEM and a smooth topography with a resolution corresponding to EGM2008 (this is because EGM2008 represents all structures below degree 2190, i.e. also the gravity effect of a smooth topography). The ultra-high frequency band is therefore taken care of by direct evaluation of the gravitational attraction caused by the masses within the RTM. We want to remind here that the aim of applying SEM is not to construct the best possible gravity field (in this case one would choose a GRACE based model for the low frequencies instead of GOCE and not simply glue the different spectral bands together), but to validate GOCE based GGFMs which requires to take care of their limited spatial resolution. Adding the short scale signal components by applying SEM is the computationally simplest approach to do so.

The SEM strategy has become attractive with the release of high-resolution GGFMs, such as GPM98A, B (Wenzel, 1998), EGM2008 (Pavlis et al., 2012) or EIGEN-6C (Förste et al., 2011). It has been used to recover various functionals of the disturbing potential, i.e. height anomalies (Hirt et al., 2010), geoid undulations (Gruber et al., 2011), deflections of the vertical (Hirt, 2010; Hirt et al., 2011), gravity disturbances (Hirt et al., 2011), gravity anomalies (Kadlec, 2011; Šprlák et al., 2012), and second order radial derivatives of the disturbing potential (Kadlec, 2011).

We have applied the SEM at all stations of our deflection database. The harmonic synthesis was performed with the GRAFIM software (Janák and Šprlák, 2006) using the low- to medium –resolution GOCE models as well as the high-resolution model EGM2008. Numerical problems of the high degree and order spherical harmonics have been avoided by implementing Horner's scheme (Holmes and Featherstone, 2002) in the GRAFIM software.

Above the resolution of EGM2008, RTM contributions have been added. The RTM was obtained as the difference between the high resolution DEMs ACE2 (Berry et al., 2010) and ASTER (Tachikawa et al., 2011) and a smooth topography, computed from topographical spherical harmonic coefficients of the elevation model DTM2006.0 (Pavlis et al., 2007). The RTM contributions to the deflections have been evaluated at each station by numerical integration. Thereby we have assumed planar approximation of the corresponding kernels. To reduce the computational time, the numerical integration has been divided into two zones, an inner and an outer zone. The inner zone makes use of $1'' \times 1''$ discretization of the mass elements as provided by the ASTER DEM. Such discretization has been applied within the integration radius $\psi = 0.1°$. Beyond that, the outer integration zone makes use of $30'' \times 30''$ discretization of the mass elements as provided by the ACE2 DEM within the integration radius $\psi = 0.5°$. Numerical experiments using variable maximum radii showed that the contribution beyond 0.5° is negligible. Throughout the numerical experiments, a standard rock density of 2670 kg m^{-3} was used for the topographic masses. The magnitude of the RTM-effect is estimated by comparison of the observations with deflections modeled from EGM2008 with and without adding the RTM-effect. The statistics are

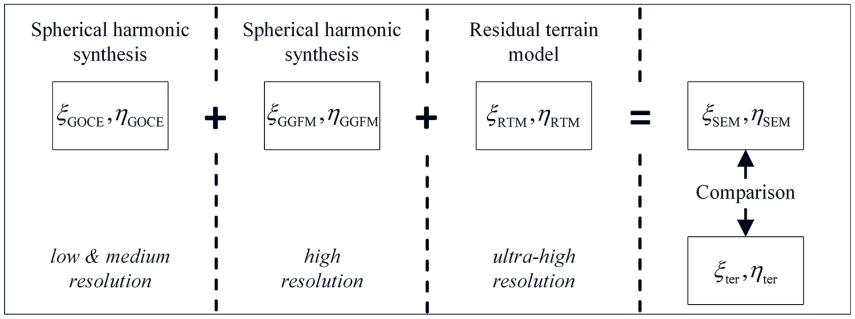

Figure 3: Schema of the spectral enhancement method (SEM).

Table 3: Statistics of the differences between observed and modeled deflections of the vertical at 110 astronomical stations in Norway (with and without consideration of the RTM-effect).

RTM	Component	min. [´´]	max. [´´]	mean [´´]	std. dev. [´´]
Not included	ξ	–5.60	9.27	–0.35	2.02
	η	–9.17	8.00	–0.76	2.39
Included	ξ	–3.44	4.40	–0.33	1.22
	η	–4.10	3.58	–0.60	1.54

shown in Table 3. The mean value roughly fits to the global average of 0.4" mentioned above. The standard deviation of the differences is reduced by almost 40% when including the RTM-effect, which compares nicely to the results by Hirt (2010) for Germany and Switzerland.

Results

In this section we present the results of our GOCE validation, i.e. the differences between observed deflections of the vertical and their modeled counterparts. In accordance with the SEM approach, the modeled deflections are based on a GOCE model up to a certain spherical harmonic degree l_{max} and the contribution of EGM2008 and a RTM above l_{max}. In order to study the quality of different spectral bands as well as the effective resolution of the GOCE models, l_{max} was successively changed from degree 2 up to the maximum degree L of each of the tested models. Figure 4 shows the standard deviations of the differences between observed and modeled deflections computed at all of the 110 stations as function of the maximum d/o l_{max} of the tested model. For example, the value of the depicted curves at degree 100 is the standard deviation of the differences which is found, when employing a specific GOCE model up to degree l_{max} = 100 and EGM2008 above degree 101. A smaller standard deviation implies better quality of the GOCE model.

In order not to overload the comparison with too many almost identical results, we restrict to some few GOCE-based models only, and relate GOCE to independent data sources by adding some GOCE-free models. The following models are considered for the comparison: EGM96 (state-of-the-art combination model before GRACE/GOCE), ITG-GRACE2010s (probably the best available pure GRACE model), the GOCE/GRACE combinations GOCO01s and GOCO03s (based on ITG-GRACE2010s and the time-wise solutions of first and third release), and the first and third release models of the direct method (DIR_r1 and DIR_r3).

The differences shown in Figure 4 are mainly caused by errors in the employed models. Errors of astronomical observations are almost one order of magnitude smaller. The model errors are largest at the higher frequ-

encies. Therefore the total model error budget is dominated by errors of EGM2008. Using only EGM2008 for all degrees provides a benchmark test which is represented by the black horizontal line in Figure 4. The standard deviation of this benchmark scenario for the SN-component (top panel) is about 1.20´´. The WE-component is at 1.47", i.e., the quality of the WE component is about 20% worse than the SN component. Replacing EGM2008 in the low- to medium spectral band by any of the other GGFMs under investigation, results in deviations from the benchmark line. Lower values, i.e. curves below the benchmark line, indicate quality improvement. The spectral/spatial resolution of the GGFMs can be defined by the maximum d/o of the model. The effective resolution, however, is given by a signal-to-noise ratio (SNR) of 1. All degrees above the effective resolution have a smaller SNR value, i.e., they contain mostly noise. This is clearly shown in Figure 4 by the fact that – above a certain degree – all curves start to deviate strongly from the benchmark line. In the sequel all curves are described in detail.

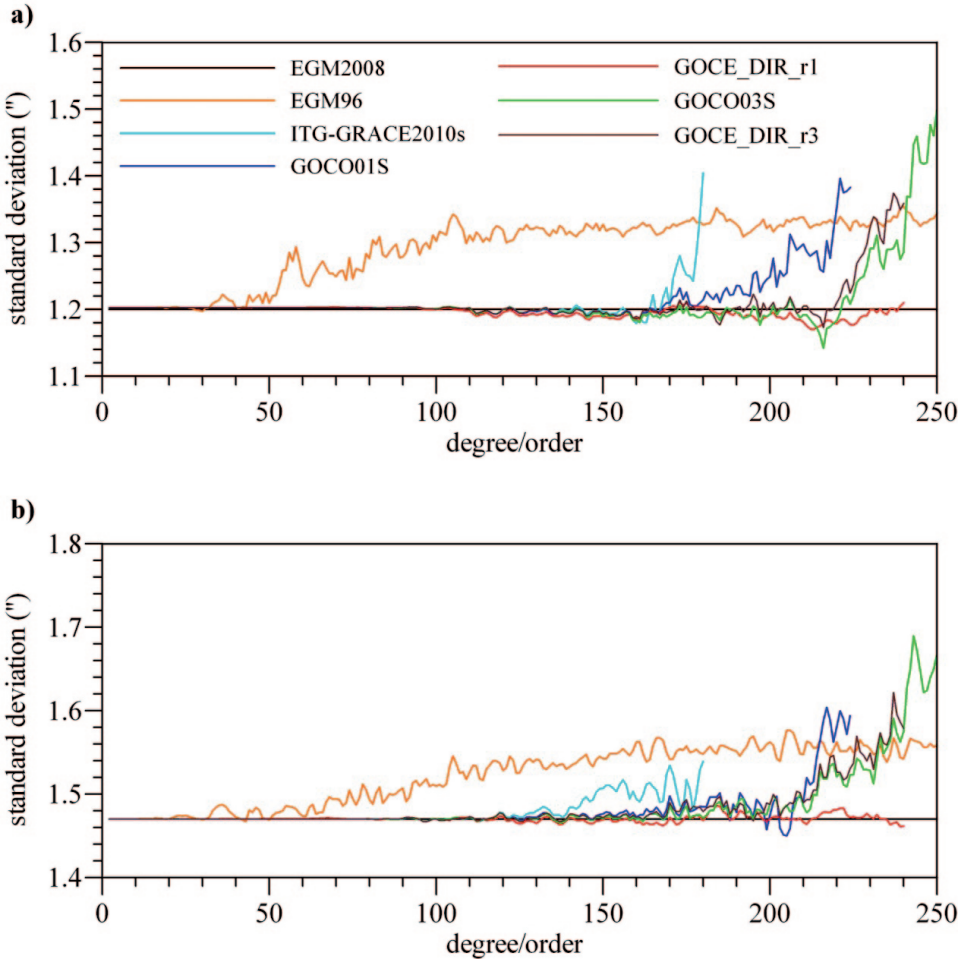

Figure 4: Standard deviation of the difference between observed and modeled deflections of the vertical for varying maximum degree l_{max} of the employed global gravity field models for (a) south-north and (b) west-east component.

EGM96 is the oldest model in our comparison. It contains satellite tracking data of various satellites acquired over several decades as well as terrestrial gravity anomalies. Below degree 50 there are only slight deviations from the benchmark line. Above this degree the standard deviations increase strongly for the NS-component and a bit less pronounced for the WE-component. After approximately degree 120 the error level stays almost constant. The lower degrees are dominated by the old satellite tracking data and also by the global average quality of terrestrial data. Higher degrees, in tendency, are more dependent on the regional quality of the terrestrial data. The constant error level above degree 120 indicates that, for the higher degrees, the error level of EGM96 is not significantly worse than for EGM2008. Indeed EGM2008 builds upon the same terrestrial database that was already used in EGM96 (Pavlis et al., 2012). It is also worthwhile to note, that the quality of the degrees below 30–50 cannot be judged from the representation in Figure 4. This is because the error budget is dominated by the higher frequencies and even significantly smaller error contributions in the low frequencies cannot change the overall error budget. Therefore one cannot recognize the tremendous increase in quality of the satellite-only solutions of GOCE and especially of GRACE as compared to the older satellite-tracking data.

The standard deviations of the NS-components for all GRACE and GOCE-based models reveal an improvement in the low and mid frequency range around degrees 110-160. Beyond this point the standard deviations of the satellite models increase by several tenths of an arc second. For ITG-GRACE2010s a significant increase at d/o 160–180 is evident while the GOCE models are significantly better in this frequency range (Gruber et al., 2011; Hirt et al., 2011). It is also interesting to note the different behavior of the NS- and the WE-components of ITG-GRACE2010s above degree 140. While the NS-deflection deviates only slightly from the benchmark line up to degree 160 and diverges strongly thereafter, the WE-deflection starts deviating already around degree 140, but does not diverge that significantly. This might be related to the error characteristics of the GRACE mission with its significant striping pattern in NS-direction (i.e., along the orbit tracks). This pattern is related to pronounced error correlations in NS-direction. Because the deflections of the vertical represent derivatives of the geoid in NS- and WE- direction, the error correlations directly influence the error budget of the deflections. Larger correlations in one direction imply smaller error estimates for the corresponding directional derivatives. Therefore one may expect the NS-error to be smaller than the WE-error due to much larger correlation lengths in NS-direction. This could explain the smaller error budget of the NS-component up to degrees around 160.

It is also interesting to note, that only two months of GOCE data (release 1) already improve solutions from seven years of GRACE data in the medium frequencies. This is more pronounced in the WE-component where GOCO01s significantly deviates from ITG-GRACE2010s.

As expected, the increase of the standard deviations of all GOCE models at higher frequencies depends on the release number. Generally, higher release number means more data and therefore better performance at higher frequencies. This is nicely illustrated by the NS-component of the GOCO models, where release 1 starts diverging at around degrees 160–170, while release 3 (with almost eight times more data than release 1) does not diverge before degree 220.

An important test for quality assessment of HPF's processing chain is to compare GOCE models based on different analysis strategies. Comparing the release 3 models of GOCO (based on the time-wise approach) and the direct approach, we see very similar error behavior. This indicates a high quality of the processing chain independent on the analysis strategy. This also confirms the results of previous studies and is in very good agreement with Šprlák et al. (2012). Theoretically, all three analysis strategies may be assumed to provide identical results. The quality of the different solutions and the differences between them thus depends crucially on the filtering of observations and the use of a priori information. This is evident from

the first release of the direct approach, which shows an exceptionally good behavior even up to the highest degrees. This is also found in the studies by Janák and Pitoňák (2011), Tscherning and Arabelos (2011), Voigt and Denker (2011) and Šprlák et al. (2012). It can be explained by the fact that DIR_r1 uses the combined model EIGEN-GL5C (Förste et al., 2008) as a priori information. The terrestrial gravity data in the a priori model causes the low error budget and prevents the error curve from diverging from the benchmark line. After recognizing the strong correlation of the final GOCE-DIR model with prior information, the satellite-only model ITG-GRACE2010s was introduced as a priori gravity field model. This prevents terrestrial gravity data from affecting the solution. The second release of the direct approach was used as a priori model for the estimation of the third release direct model DIR_r3. This shows the importance of the proper choice of prior information and that a reasonable choice of a priori information in the direct method leads to a competitive performance with respect to the time-wise solution. It should be mentioned that integration of a priori information is in the time-wise models limited to regularization of the high frequencies of the spectra above degree 180 applying Kaula's degree variance model (Kaula, 1966). This gives a rough estimate of the expected average size of spherical harmonic coefficients of a certain degree and helps to smooth the noise contribution in the high frequencies.

Overall, the level of improvement brought by different releases of GOCE models is approximately equal for both the SN and the WE component. However, the level is four times smaller than reported by Voigt and Denker (2011) and two times smaller than observed by Šprlák et al. (2012). The discrepancies with respect to Voigt and Denker (2011), who performed their study with deflections of the vertical in Germany, might be caused by the different geographic locations of the study area (see e.g. Šprlák et al., 2012). The less pronounced improvements with respect to (Šprlák et al., 2012), who validated GOCE models over Norway using gravity anomalies, might be caused by different spectral characteristics of different gravity field functionals.

Regional modeling of the gravity field

Many geodetic applications require high resolution gravity field information. Therefore, regional refinements of global models – such as those derived from GOCE – are necessary. Classical techniques for such a regional gravity field modeling are the integration of terrestrial gravity anomalies by means of Stokes's equation

$$N(P) = \frac{R}{4\pi\gamma} \iint_{\sigma} S(\psi_{PQ})\, \Delta g_Q \, \mathrm{d}\sigma_Q \qquad (5)$$

and least-squares collocation, which provides an optimal estimation of arbitrary gravity field quantities from various point observations in a statistical sense. It employs knowledge of the signal covariance and tries to minimize the prediction error. If we restrict ourselves to a comparison with Stokes's equation, i.e. with the estimation of geoid heights from gravity anomalies, collocation can be written in the following way

$$N(P) = C_{Pi}^{Ng} \left(C_{ij}^{gg} \right)^{-1} \Delta g_i \,, \qquad (6)$$

where matrices C contain signal covariances between the functionals indicated in the superindex at locations indicated in the index; in that sense C_{Pi}^{Ng} represent cross-covariances between gravity anomalies and geoid heights between the points i of the input data and computation point P.

Both methods can be applied globally. However, due to the large number of gravity points available, collocation requires huge computational efforts when applied to larger data sets. In practice both methods are applied regionally and only the residual geoid with respect to a long wavelength reference model is approximated. In the case of Stokes the global model is necessary because equation (5) requires global integration, which for the largest signal contribution is implicitly included in the reference model. In case of collocation, the statistical setup requires the residual signal to be of stochastic nature without deterministic components such as trends or periodic oscillations. Such deterministic components are reduced by computation of residual quantities. The use of global reference models also allows

restricting the use of terrestrial data to a limited region. Usually the reference models are provided in terms of spherical harmonics. From a set of spherical harmonic coefficients $\{\Delta\bar{C}_{lm}, \Delta\bar{S}_{lm}\}$ of the disturbing potential, the geoid can be computed according to

$$N(P) = R\sum_{l=2}^{L}\sum_{m=0}^{l}\left(\Delta\bar{C}_{lm}\cos m\lambda_P + \Delta\bar{S}_{lm}\sin m\lambda_P\right)\bar{P}_{lm}(\cos\theta_P). \quad (7)$$

All of the three classical methods/parameterizations (equations (5)–(7)) are identical if applied globally. This holds true for Stokes's integral and the spherical harmonic representation (see Heiskanen and Moritz, 1967), but may also be shown for Stokes integral and collocation. Following the interpretation in de Min (1995), the gravity anomalies used in Stokes's integral (integration elements at point Q) are predicted from point gravity values observed at discrete location i by means of collocation. Then Stokes's equation can be written as

$$\begin{aligned} N(P) &= \frac{R}{4\pi\gamma}\iint_{\sigma} S(\psi_{PQ})\,\Delta g_Q\,\mathrm{d}\sigma_Q \\ &= \frac{R}{4\pi\gamma}\iint_{\sigma} S(\psi_{PQ})\left[C_{Qi}^{gg}\left(C_{ij}^{gg}\right)^{-1}\Delta g_i\right]\mathrm{d}\sigma_Q \end{aligned} \quad (8)$$

and because the original gravity stations i do not depend on the integration element

$$N(P) = \frac{R}{4\pi\gamma}\left[\iint_{\sigma} S(\psi)C_{Qi}^{gg}\,\mathrm{d}\sigma_Q\right]\left(C_{ij}^{gg}\right)^{-1}\Delta g_i\,. \quad (9)$$

Both of the functions inside of the integral can be written in terms of Legendre series, i.e.

$$S(\psi_{PQ}) = \sum_{l=2}^{\infty}\frac{2l+1}{l-1}P_l\left(\cos\psi_{PQ}\right) \quad (10)$$

$$C_{Qi}^{gg} = \sum_{l=2}^{\infty} c_l P_l\left(\cos\psi_{Qi}\right), \quad (11)$$

with c_l being the signal degree variances of the residual gravity anomalies and $P_l\left(\cos\psi_{Qi}\right)$ are the Legendre polynomials. Insertion of equation (10) and (11) into (9) and application of decomposition theorem and orthogonality relations of spherical harmonics (see Heiskanen and Moritz, 1967) yields

$$\begin{aligned} N &= \frac{R}{4\pi\gamma}\left[\iint_{\sigma}\sum_{l=2}^{\infty}\frac{2l+1}{l-1}P_l\left(\cos\psi_{PQ}\right)\cdot\sum_{l=2}^{\infty}c_l P_l\left(\cos\psi_{Qi}\right)\mathrm{d}\sigma_Q\right]\left(C_{ij}^{gg}\right)^{-1}\Delta g_i \\ &= \sum_{l=2}^{\infty}\left[\frac{R}{\gamma(l-1)}c_l P_l\left(\cos\psi_{Pi}\right)\right]\left(C_{ij}^{gg}\right)^{-1}\Delta g_i \\ &= C_{Pi}^{Ng}\left(C_{ij}^{gg}\right)^{-1}\Delta g_i. \end{aligned} \quad (12)$$

This derivation shows that Stokes integral and collocation are identical, if applied globally. Thereby, collocation is interpreted as a two step procedure. In the first step gravity anomalies are predicted continuously over the entire Earth's surface from given point gravity data in the area of interest. In the second step Stokes's integration of this continuous data set of predicted gravity anomalies is performed globally. However, de Min (1995) points out that the two methods are not identical in regional applications. This is because Stokes's integration can easily be restricted to a spherical cap around the computation point (with no data from outside the cap being used), while collocation implicitly takes the contribution from outside the cap into account. This however is not desired because the data in the far zone does not reflect the actual gravity field outside the cap, but is only derived by extrapolation of the data inside the cap. The problem can be overcome by proper modification of the cross-covariance function C^{Ng} (which is equivalent to a modification of the Stokes kernel) such that both methods become identical.

Besides these classical methods spherical wavelet representations – or generally the use of spherical radial basis functions – have become popular since several years, see e.g. Freeden and Schreiner (2005), Panet et al.

(2005), Schmidt et al. (2007), Tenzer and Klees (2007) or Antoni et al. (2009). Such approaches can be interpreted as spectral representations (based on spherical harmonics) which are limited to a certain spatial region only. Similar to the signal covariance functions used in collocation, the radial basis functions depend on a specific location (origin) and the spherical distance between this origin and the actual computation point. In contrast, the spherical harmonic basis functions $\bar{P}_{lm}(\cos\theta_P)\cos m\lambda_P$ and $\bar{P}_{lm}(\cos\theta_P)\sin m\lambda_P$ only depend on the computation point P. This is reflected in the amplitude of the oscillations of the basis functions, which are shown in Figure 5. The amplitude is constant all around the globe in the case of spherical harmonics (mid panel in Figure 5). In the case of radial basis functions (right panel in Figure 5) the amplitude is strongly diminished with increasing distance from the origin. Therefore the influence of a radial basis function on very distant points is practically zero, which makes them suitable for regional gravity field modeling. One says that spherical harmonics have *global support*, while radial basis functions have quasi[4] *local support*. Spherical harmonics, which have global support in the spatial domain, are related to one single combination of degree and order numbers {*l*,*m*}, i.e. they are related to exactly one spectral line and therefore are perfectly localizing in the spectral domain. Perfect localization in either the spectral or the spatial domain goes hand-in-hand with no localization in the other domain. Perfect localization in both domains is not possible. Spherical harmonics are an extreme example of having perfect frequency localization, but no spatial localization. The other extreme, no frequency localization but perfect spatial localization is given by the Dirac-function with infinite amplitude at the origin and zero amplitude at all other locations. Wavelets or radial basis functions represent a compromise. They are quasi-localizing in the spatial domain at the cost of spreading the spectral content over a wider range of spectral lines, or spherical harmonic degrees (see Figure 6).

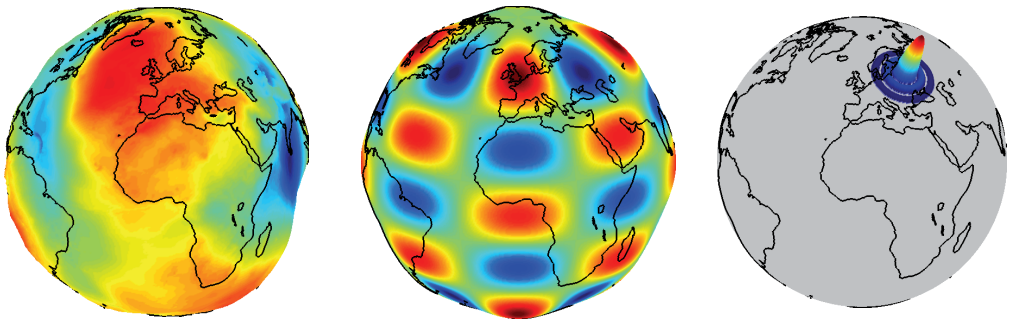

Figure 5: The global geoid (left) can be constructed from a superposition of spherical harmonic basis functions (middle) or of quasi space localizing radial basis functions (right). The middle panel shows a tesseral spherical harmonic function of degree l=8 and order m=4. The right panel shows a Blackman scaling function located at the origin with spherical coordinates λ=30° and φ=55°.

Independent of their localization properties, it can be shown that representations in spherical harmonics and in radial basis functions are mathematically equivalent – at least if the latter are distributed evenly around the globe. This is shown in the following equations. For the sake of compactness of the equations, we use complex notation for spherical harmonics with the order number m covering all degrees in the range $\{-l;\, l\}$ and

$$Y_{lm}^{R} = \frac{1}{R\sqrt{4\pi}}\,\bar{P}_{l|m|}(\cos\theta_P)\cdot\begin{cases}\cos m\lambda_P\\ \sin|m|\lambda_P\end{cases}$$

$$\text{for } m = \begin{cases} 0,\ldots,l\\ -l,\ldots,-1\end{cases}$$

4. The amplitude is very small for large distances from the origin, but not exactly zero. Therefore the support is not actually local, but only quasi-local.

$$c_{lm} = \sqrt{4\pi}\,GM \cdot \begin{cases} \bar{C}_{lm} \\ \bar{S}_{lm} \end{cases} \quad \text{for } m = \begin{cases} 0,\ldots,l \\ -l,\ldots,-1 \end{cases}.$$

In this notation, the spherical harmonic series expression of the gravitational potential (cf. equation (1)) is given by

$$V(P) = \sum_{l=0}^{\infty} \left(\frac{R}{r_P}\right)^{l+1} \sum_{m=-l}^{l} c_{lm}\, Y_{lm}^{R}(P). \qquad (13)$$

Thereby the spectral coefficients c_{lm} may be derived by spherical harmonic analysis, i.e. from the global integration of the product between signal (the potential function V given at points Q on the surface of the sphere) and the basis function Y_{lm}^{R} of the corresponding degree and order numbers l and m. Inserting this into equation (13) yields

$$V(P) = \sum_{l=0}^{\infty} \left(\frac{R}{r_P}\right)^{l+1} \cdot \sum_{m=-l}^{l} \left[\int_{\Omega_Q} V(Q) Y_{lm}^{R}(Q)\, d\Omega_Q \right] Y_{lm}^{R}(P)\,, \qquad (14)$$

and after interchanging the order of summation and integration and employing the addition theorem of spherical harmonics (see Heiskanen and Moritz, 1967)

$$V(P) = \int_{\Omega_Q} V(Q) \left[\sum_{l=0}^{\infty} \left(\frac{R}{r_P}\right)^{l+1} \cdot \sum_{m=-l}^{l} Y_{lm}^{R}(Q) \cdot Y_{lm}^{R}(P) \right] \mathrm{d}\Omega_Q$$

$$= \int_{\Omega_Q} V(Q) \left[\sum_{l=0}^{\infty} \left(\frac{R}{r_P}\right)^{l+1} \cdot \frac{2l+1}{4\pi R^2} P_l\left(\cos\psi_{PQ}\right) \right] \mathrm{d}\Omega_Q. \qquad (15)$$

Introducing the Abel-Poisson kernel function

$$k_{AP}(P,Q) = \sum_{l=0}^{\infty} \frac{2l+1}{4\pi R^2} \left(\frac{R}{r}\right)^{l+1} P_l(\cos\psi_{PQ}) \qquad (16)$$

we may write

$$V(P) = \int_{\Omega_Q} k_{AP}(P,Q)\, V(Q)\, \mathrm{d}\Omega_Q. \qquad (17)$$

This is a convolution of the potential V, given at the surface of the sphere (at points Q) with the kernel function $k_{AP}(P,Q)$ between points P and Q. In symbolic notation the convolution can be written as

$$V(P) = \left(k_{AP} * V\right)_{\Omega_Q}\left(\underline{x}_P\right). \qquad (18)$$

The derivation shows, that convolution with a proper kernel function is equivalent to the spherical harmonic representation of equation (13). The convolution formula (17) is also equivalent to the well known Poisson integral (Heiskanen and Moritz, 1967)

$$V(P) = \int_{\Omega_Q} \frac{R(r_P^2 - R^2)}{4\pi s^3}\, V(Q)\, \mathrm{d}\Omega_Q \qquad (19)$$

where s is the distance between points P and Q, i.e. $s = \sqrt{r_P^2 + R^2 - 2Rr_P\cos\psi_{PQ}}$.

It is important to note that convolution with the Abel-Poisson kernel k_{AP} gives the original signal. The kernel is a reproducing kernel. There is a wide range of kernels which have interesting properties for regional gravity field modeling. Generalizing the representation of the Abel-Poisson kernel in equation (16), we may write the general kernel function $B(P,Q)$ as

$$B(P,Q) = \sum_{l=0}^{\infty} \frac{2l+1}{4\pi R^2} \left(\frac{R}{r}\right)^{l+1} B_l P_l(\cos\psi_{PQ}), \qquad (20)$$

where the coefficients B_l define the characteristics of the kernel function. All kernel functions of this type are isotropic functions, because they depend only on the spherical distance ψ_{PQ} between the points P and Q. Thus they are called radial basis functions. Comparison of equations (16) and (20) shows that $B_l = 1$ for all degrees l of the Abel-Poisson kernel. Modification of the B_l-coefficients changes the spectral characteristics as well

as the spatial shape of the kernel function. Several radial basis functions as well as the corresponding B_l-coefficients are shown in Figure 6. The spectral representation reveals that the modification of the B_l-coefficients corresponds to signal filtering. Thereby low-pass (right column in Figure 6) and band-pass (left column) filtering is possible. In connection with wavelet theory, band-pass filtering is provided by wavelet functions, which cover only a certain spectral band. Low-pass filtering is provided by scaling functions, which represent the superposition of wavelets from different spectral bands. The examples shown in Figure 6 cover scaling and wavelet functions of type Shannon, Blackman and Poisson multipole as well as a cubic polynomial and the Abel-Poisson kernel. They have been discussed in Freeden et al. (1998), Freeden and Michel (2004), Holschneider et al. (2003), Chambodut et al. (2005), Panet et al. (2005), Schmidt et al. (2006), Schmidt et al. (2007), Tenzer and Klees (2007), Eicker (2008), Klees et al. (2008), Antoni et al. (2009) and Panet et al. (2010) amongst many others.

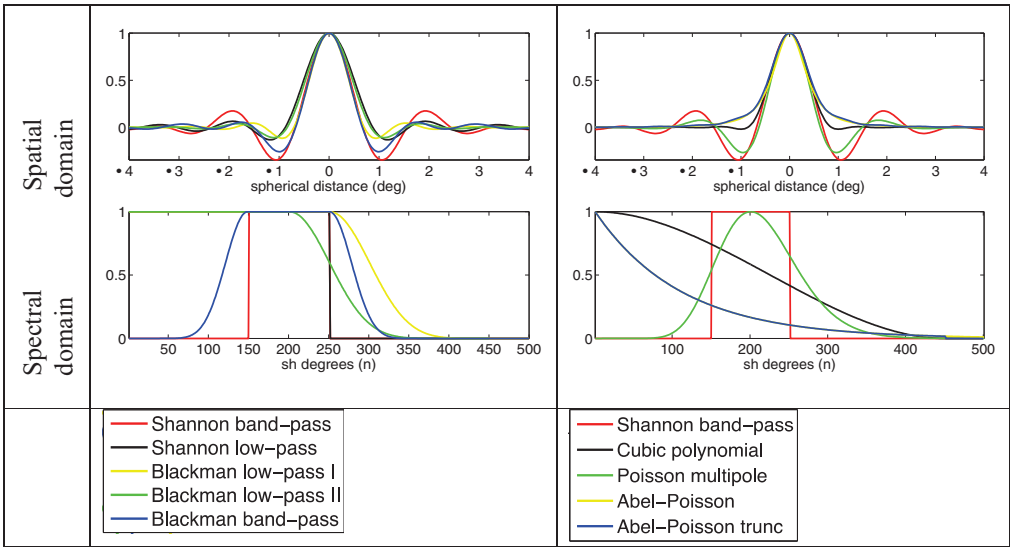

Figure 6: Spatial (upper panels) and spectral (lower panels) representation of different types of band-pass (wavelet) and low-pass (scaling) functions.

The spatial characteristics in the upper row of Figure 6 show that all of the basis functions oscillate around zero, have the largest amplitude at the origin and drop to relatively small values with increasing distance from the origin. This is similar to collocation, where the signal covariance function has the largest amplitude at the origin (the signal variance) and drops towards zero for increasing distance. Therefore, in both cases, data points near the origin have the strongest influence on the modeling result, while data in remote zones play a minor role. However, restricting gravity field modeling to local or regional scales still leads to truncation errors, which cannot be avoided, and which are more or less significant depending on the size of the study area, the spectral characteristics of the signal as well as on the chosen basis function.

Most of the functions in Figure 6 show a smooth transition in the spectral domain (lower panels) from values of one to zero. Only the Shannon wavelet (band-pass) shows a sharp transition. It exactly (and completely) cuts a certain band from the spherical harmonic degree spectrum. Therefore, in a global gravity field representation, a band-limited signal can be exactly represented with the Shannon wavelet, provided that the mi-

nimum and maximum degree of the Shannon wavelet coincides with the minimum and maximum degree of the signal. As shown in equation (17), convolution with the Abel-Poisson kernel reproduces the non band-limited gravity signal exactly. However, convolution requires a continuous and complete coverage of and integration over the whole globe. Because this is numerically not possible, there is an approximation error. Furthermore, truncation errors arise from restricting the computations to local or regional scales, as discussed above. Additionally, if we assume a gravity signal in the bandwidth from, e.g., spherical harmonic degree 150 to 250 (this corresponds to the pass-band of the Shannon wavelet in Figure 6), not all of the radial basis functions presented in Figure 6 can reproduce the full spectral content of the signal due to their spectral characteristics (limited frequency localization). But because the radial basis functions are a compromise between localization in the spatial and spectral domain, making only use of the spectral characteristics for assessment of the modeling quality is not advisable. Indeed, validations of modeling results show that functions which are smooth both in the spatial and frequency domains lead to better modeling results than, e.g., the Shannon band-pass function. Even though the latter exactly covers the signal bandwidth in the spectral domain, it has the highest side-lobes and oscillations in the spatial domain which is unfavorable considering space-localizing requirements in regional modeling.

In the sequel we present a synthetic example of regional gravity field modeling. Thereby a closed-loop model is set up to test the quality of regional modeling. In the first step (estimation), synthetic data is generated from a spherical harmonic input model and used to derive a regional gravity field model. In the second step (validation) the regional field is compared to values derived from the input model at an independent set of validation points. The difference between the two representations is the empirical error of the regional modeling. The linear observation model employed in the estimation step is based upon the following mathematical consideration: if two functions are in the same function space, then the result of their convolution is as well in the same space. In our case, the gravitational potential $V(Q)$ and the kernel $B(P,Q)$ are in the linear space of square integrable functions L_2 on the sphere. Therefore also the result of the convolution $V \cdot B$ is in L_2 on the sphere and can be represented as linear combination of a set of kernel functions $B(P,Q)$ (which span L_2), located on a regular grid with k grid points Q_k covering the area of interest. It holds

$$\begin{aligned} V(P) &= \left(B * V\right)_{\Omega_Q}\left(\underline{x}_P\right) \\ &= \sum_{k=1}^{\infty} d_k B(P,Q_k) \approx \sum_{k=1}^{K} d_k B(P,Q_k) \end{aligned} \tag{21}$$

from which the linear observation model

$$\mathbf{y}(P) + \mathbf{e}(P) = \mathbf{B}(P,Q_k)^T \cdot \mathbf{d}_k \tag{22}$$

is derived. Thereby the elements of the design matrix are computed from the kernel function and the coefficient vector $\boldsymbol{d}_k$ contains the unknowns. Given gravity field observations at data points P and the distribution of grid points Q_k, the unknown coefficients can be estimated in least-squares sense. This also allows for a proper description of the formal error of the d_k coefficients and error propagation to arbitrary gravity field quantities. The estimation model can be extended to combine different types of observations, like geoid heights, gravity anomalies, gravity gradients in orbit height, etc. In addition, proper selection and/or modification of the kernel function allows spectral filtering.

The results of our synthetic example are shown in Figure 7. The Shannon low-pass function is used for gravity field representation. The study area is located in the Himalaya region between 27° and 33° latitude and 77° and 88° longitude. The signal is shown in the left panel of Figure 7 and represents the gravitational potential in the bandwidth between spherical harmonic degrees 150 and 250. The empirical error of the regional model is shown in the right panel of in Figure 7. The relative empirical error has an RMS value of only $1.2 \cdot 10^{-5}$ which corresponds to 12 µm in terms of geoid heights. Using other types of radial

basis functions, this error can be further reduced. The cubic polynomial or Poisson multipole kernels yield about two orders of magnitude smaller errors. The relative empirical error has an RMS of the order of 10^{-7}.

It is worthwhile to note, that the spherical harmonic representation of the signal contains 40200 coefficients, while for the regional representation only 1437 coefficients are needed. Because radial basis functions are only required in the area of interest (including some margin to minimize truncation errors) the number of coefficients used to represent the signal is relatively small. Therefore they allow very detailed refinements in the area of interest with moderate numerical effort.

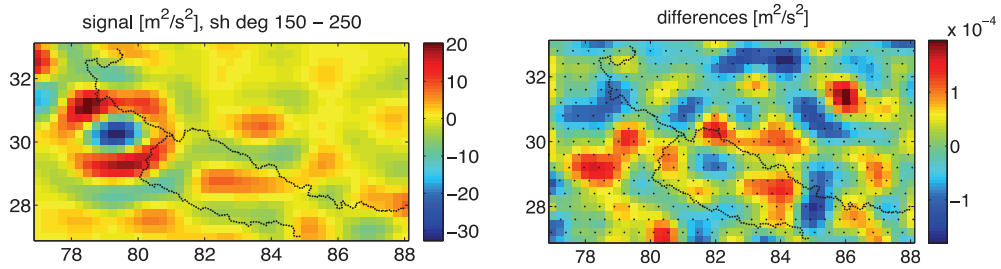

Figure 7: Gravitational potential in the Himalaya region in the spectral range between spherical harmonic degrees 150 and 250 (left) and the empirical error (right) of a corresponding regional gravity field model based on Shannon band-pass basis functions.

Summary and conclusions

Drawing historical lines from the beginning of Norwegian gravity field research in the 1860ies, current research topics at the Norwegian University of Environmental and Life Sciences are presented. We have validated ESA's satellite gravimetry mission GOCE with historic astronomical observations in Norway, many of which Olav Mathisen had measured. The comparison shows the high quality of GOCE data products in general, but also reveals differences in processing strategies. Global gravity field models, like those based on GOCE, act as long-wavelength reference models for regional refinements. Besides the classical methods like Stokes integration and collocation, today, also spherical wavelet-type representations are investigated. We have described the general concept and shown that regional modeling is possible with very high accuracy. Advantages of representations in radial basis functions are their spectral form which allows data filtering, the quasi-local support which allows restriction of the modeling to the region of interest and the formulation in terms of a linear observation model. This allows combination of different types of gravity field observations and the derivation of proper error measures. The limitation of the study region makes the estimation efficient and keeps the numerical effort on a moderate level.

Acknowledgements

Kartverket is gratefully acknowledged for providing the database of vertical deflections in Norway. Michael Schmidt of DGFI in Munich is gratefully acknowledged for discussions on radial basis functions. Last but not least, we thank Olav Mathisen for his continuing and inspiring guidance of students and colleagues at UMB.

References

Antoni, M., Keller, W., and Weigelt, M., 2009, Representation of Regional Gravity Fields by Radial Base Functions. In: Sideris, M.G. (red.) *Observing our Changing Earth*. IAG Symposia, Vol. 133, 293–299. Springer Berlin Heidelberg.

Berry, P.A.M., Smith, R.G., Benveniste, J., 2010, ACE2: The new global digital elevation model. In: Mertikas S.P. (Ed.), *Gravity, Geoid and Earth Observation*, IAG Symposia, Vol. 135, 23–27 June 2008, Chania, Greece, p. 231–238.

Blankenburgh, J. C., 1987, Geodesi med stjerner og satellitter i Norge. *Bilag til Kart og Plan* nr. 1 – 1987, p. 91–95.

Breili, K., Gjevestad, J. G., Lysaker, D. I., Omang, O. C. D., Pettersen, B. R., 2010, Absolute gravity values in Norway. *Norwegian Journal of Geography* **64**, 79–84.

Bruinsma, S.L., Marty, J. C., Balmino, G., Biancale, R., Foerste, C., Abrikosov, O., and Neumayer, H., 2010, GOCE Gravity Field Recovery by Means of the Direct Numerical Method, presented at the ESA Living Planet Symposium 2010, Bergen, June 27–July 2 2010, Bergen, Norway.

Chambodut, A., Panet, I., Mandea, M., Diament, M., Holschneider, M., and Jamet, O., 2005, Wavelet frames: an alternative to spherical harmonic representation of potential fields. *Geophysical Journal International, 163*, 875–899.

Danielsen, J., Sundsby, J., 1995, Målinger med senitkamera for loddavvik. Faglig melding, Geodesidivisjonen, Statens kartverk.

Drewes, H., 2012, Current Activities of the International Association of Geodesy (IAG) as the Successor Organisation of the Mitteleuropäische Gradmessung. *ZfV*, 137(3).

ESA, 1999, Gravity Field and Steady-State Ocean Circulation Mission. ESA SP-1233(1), report for mission selection of the four candidate Earth Explorer missions.

Eicker, A., 2008, Gravity Field Refinement by Radial Basis Functions from In-situ Satellite Data. Dissertation, Institut für Geodäsie und Geoinformation, Universitity Bonn, Germany.

Flury, J., 2005, Short-wavelength Spectral Properties of the Gravity Field from a Range of Regional Data Sets. *Journal of Geodesy*, 79(10–11), 624–640, doi: 10.1007/s00190-005-0011-y.

Forsberg, R., 1984, A study of terrain reductions, density anomalies and geophysical inversion methods in gravity field modeling. Report No. 355, Department of Geodetic Science and Surveying, Ohio State University, Columbus, USA.

Förste, C., Bruinsma, S., Shako, R., Marty, J.-C., Flechtner, F., Abrikosov, O., Dahle, C., Lemoine, J.-M., Neumayer, H., Biancale, R., Barthelmes, F., König, R., and Balmino, G., 2011, EIGEN-6 – A new combined global gravity field model including GOCE data from the collaboration of GFZ-Potsdam and GRGS-Toulouse. *Geophysical Research Abstracts*, Vol. 13, EGU2011-3242-2, EGU General Assembly 2011.

Freeden, W., Gervens, T., and Schreiner, M., 1998, *Constructive Approximation on the Sphere With Applications to Geoscience*. Oxford Science Publications.

Freeden, W., and Michel, V., 2004, *Multiscale Potential Theory With Applications to Geoscience*. Springer Basel AG.

Freeden, W., and Schreiner, M., 2005, Spaceborne gravitational field determination by means of locally supported wavelets. *Journal of Geodesy, 79*, 431–446.

Gauss, C. F., 1828, *Bestimmung des Breitenunterschiedes zwischen den Sternwarten von Göttingen und Altona durch Beobachtungen am Ramsdenschen Zenithsector.* Vandenhoeck und Ruprecht, Göttingen.

Gruber, T., Visser, P.N.A.M., Ackermann, C., Hosse, M., 2011, Validation of GOCE gravity field models by means of orbit residuals and geoid comparisons. *Journal of Geodesy*, **85**, p. 845–860.

Guimarãeas, G.N., Matos, A.C.O.C., Blitzkow, D., 2012, An evaluation of recent GOCE geopotential models in Brazil. *Journal of Geodetic Science*, **2**, p. 144–155.

Hansteen, C., 1825, Capt. Sabines Pendel-Iagttagelser. *Magazin for Naturvidenskaberne* **6**, 309–310.

Heiskanen, W., and Moritz, H., 1967, Physical Geodesy. Freeman, San Francisco.

Hirt, C., 2010, Prediction of vertical deflections from high-degree spherical harmonic synthesis and residual terrain model data. *Journal of Geodesy*, **84**, p. 179–190.

Hirt, C., Featherstone, W.E., Marti, U., 2010, Combining EGM2008 and SRTM/DTM2006.0 residual terrain model data to improve quasigeoid computations in mountainous areas devoid of gravity data. *Journal of Geodesy*, **84**, p. 557–567.

Hirt, C., Gruber, T., Featherstone, W.E., 2011, Evaluation of the first GOCE static gravity field models using terrestrial gravity, vertical deflections and EGM2008 quasigeoid heights. *Journal of Geodesy*, **85**, p. 723–740.

Holmes, S.A., Featherstone, W.E., 2002, A unified approach to the Clenshaw summation and the recursive computation of very high degree and order normalized associated Legendre functions. *Journal of Geodesy*, **76**, p. 279–299.

Holschneider, M., Chambodut, A., and Mandea, M., 2003, From global to regional analysis of the magnetic field on the sphere using wavelet frames. *Physics of the Earth and Planetary Interiors, 135*, 107–124.

Janák, J., Šprlák, M., 2006, A new software for gravity field modeling. *Geodetic and Cartographic Horizon*, **52**, p. 1–8 (in Slovak).

Janák, J., Pitoňák, M., 2011, Comparison and testing of GOCE global gravity models in central Europe. *Journal of Geodetic Science*, **1**, p. 333–347.

Jekeli, C., 1999, An analysis of vertical deflections derived from high-degree spherical harmonic models. *Journal of Geodesy*, **73**, p. 10–22.

Jelstrup, H.J., 1929, Determinations of astronomical longitudes, latitudes and azimuths. *Geodetiske arbeider*, hefte II (1929) og III (1931), Norges geografiske opmåling.

Kaula, W., 1966, *Theory of satellite geodesy*. Blaisdell Pub. Co., Waltham, Massachusetts.

Kadlec, M., 2011, Refining gravity field parameters by residual terrain modeling. Doctoral Thesis, Department of Mathematics, Faculty of Applied Sciences, University of West Bohemia, Pilsen, Czech Republic, 150 p.

Klees, R., Tenzer, R., Prutkin, I., and Wittwer, T., 2008, A data-driven approach to local gravity field modelling using spherical radial basis functions. *Journal of Geodesy, 82*, 457–471.

Koop, R., Visser, P.N.A.M., Tscherning, C.C., 2001, Aspects of GOCE calibration. In: *Proceedings of the International GOCE User Workshop*, WPP-188, ESA/ESTEC, Noordwijk, Netherlands, p. 51–56.

Kühnen, F. J., Furtwängler, P., 1906, Bestimmung der absoluten Grösze der Schwerkraft zu Potsdam mit Reversionspendeln. Veröff. kgl. preuss. geodät. Inst., N.F., Nr. 27.

Listing, J. B., 1873, Über unsere jetzige Kenntnis der Gestalt und Größe der Erde. Nachrichten der Königlichen Gesellschaft der Wissenschaften und der Georg-August-Universität, 33–98, Göttingen.

Lemoine, F.G., Kenyon, S.C., Factor, J.K., Trimmer, R.G., Pavlis, N.K., Chin, D.S., Cox, C.M., Klosko, S.M., Luthcke, S.B., Torrence, M.H., Wang, Y.M., Williamson, R.G., Pavlis, E.C., Rapp, R.H., Olson, T.R., 1998. The development of the joint NASA GSFC and NIMA geopotential model EGM96. NASA Technical Report 1998-206861, NASA/GSFC, Greenbelt, USA.

Mayer-Gürr, T., Rieser, D., Höck, E., Brockmann, J.M., Schuh, W.D., Krasbutter, I., Kusche, J., Maier, A., Krauss, S., Hausleitner, W., Baur, O., Jäggi, A., Meyer, U., Prange, L., Pail, R., Fecher, T., Gruber, T., 2012, The new combined satellite only model GOCO03s. Abstract submitted to GGHS2012, Venice (Poster).

Migliaccio, F., Reguzzoni, M., Sansó, F., Tscherning, C.C., Veicherts, M., 2010, GOCE data analysis: the space-wise approach and the first space-wise gravity field model. In: *Proceedings of the ESA Living Planet Symposium*, 28 June–2 July 2010, Bergen, Norway.

de Min, E., 1995, A comparison of Stokes's numerical integration and collocation, and a new combination technique. *Bull. Géod.*, 69: 233–232.

Pail, R., Goiginger, H., Schuh, W.D., Höck, E., Brockmann, J.M., Fecher, T., Gruber, T., Mayer-Gürr, T., Kusche, J., Jäggi, A., Rieser, D., 2010, Combined satellite gravity field model GOCO01S derived from GOCE and GRACE. *Geophysical Research Letters*, **37**, L20314, doi:10.1029/2010GL044906.

Pail, R., Bruinsma, S., Migliaccio, F., Förste, C., Goiginger, H., Schuh, W.D., Höck, E., Reguzzoni, M., Brockmann, J.M., Abrikosov, O., Veicherts, M., Fecher, T., Mayrhofer, R., Krasbutter, I., Sansó, F., Tscherning, C.C., 2011, First GOCE gravity field models derived by three different approaches. *Journal of Geodesy*, **85**, p. 819–843.

Panet, I., Jamet, O., Diament, M., and Chambodut, A., 2005, Modelling the Earth's gravity field using wavelet frames. In: Jekeli, C., Bastos, L., Fernandes J. (eds.) *Gravity, Geoid and Space Missions*. IAG Symposia, Vol. 129, pp. 48–53. Springer Berlin Heidelberg.

Panet, I., Kuroishi, Y., and Holschneider, M., 2010, Wavelet modelling of the gravity field by domain decomposition methods: an example over Japan. *Geophysical Journal International, 184*, 203–219.

Pavlis, N.K., Factor, J.K., Holmes, S.A., 2007, Terrain-related gravimetric quantities computed for the next EGM. In: Gravity Field of the Earth, Proceedings of the 1st International Symposium of the International Gravity Field Service, Harita Dergisi, Special Issue 18, Istanbul, Turkey, p. 318–323.

Pavlis, N. K., Holmes, S. A., Kenyon, S. C., Factor, J. K., 2012, The development and evaluation of the Earth Gravitational Model 2008

(EGM2008). *J. Geophys. Res.*, Vol. 117, B04406, 38 PP., doi:10.1029/2011JB008916.

Pettersen, B. R., 2002, Christopher Hansteen and the first observatory at the University of Oslo, 1815–28. *Journal of Astronomical History and Heritage* **5**(2): 123–134.

Pettersen, B. R., 2006, Christopher Hansteens rolle i geodesiens utvikling i Norge. I. Utvikling av en toposentrisk, astrogeodetisk, nasjonal referanseramme, 1815–1865. *Kart og Plan*, Vol. 66, pp. 171–180.

Pettersen, B. R., 2007, Christopher Hansteens rolle i geodesiens utvikling i Norge. II. Vitenskapelige gradmålinger. *Kart og Plan*, Vol. 67, pp. 38–46.

Pettersen, B. R., 2009, The first astro-geodetic reference frame in Norway, 1779–1815. *Acta Geod. Geoph. Hung.*, Vol. 44(1), pp. 67–78. DOI:10.1556/AGeod.44.2009.1.7.

Rummel, R., Gruber, T., Koop, R., 2004, High Level Processing Facility for GOCE: products and processing strategy. In: Lacoste, H. (ed.) Proceedings of the 2nd International GOCE User Workshop "GOCE, The Geoid and Oceanography", ESA SP-569, ESA.

Sabine, E., 1825, *An account of experiments to determine the figure of the Earth by means of the pendulum vibrating seconds in different latitudes.* London 1825.

Schiøtz, O. E., 1894, Resultate der im Sommer 1893 in dem nördlichsten Theile Norwegens ausgeführten Pendelbeobachtungen nebst einer Untersuchung über den Einfluss von Bodenerschütterungen auf die Schwingungszeit eines Pendels. Norwegische Commission der Europäischen Gradmessung, Kristiania 1894.

Schiøtz, O. E., 1895, Resultate der im Sommer 1894 in dem südlichsten Theile Norwegens ausgeführten Pendelbeobachtungen. Norwegische Commission der Europäischen Gradmessung, Kristiania 1895.

Schmidt, M., Fengler, M., Mayer-Gürr, T., Eicker, A., Kusche, J., Sanchez, L., and Han, S.-C., 2007, Regional Gravity Modeling in Terms of Spherical Base Functions. *J. Geodesy, 81*, 17–38.

Šprlák, M., Gerlach, C., Omang, O.C.D., Pettersen, B.R., 2011, Comparison of GOCE derived satellite global gravity models with EGM2008, the OCTAS geoid and terrestrial gravity data: case study for Norway. In: Proceedings of the 4th International GOCE User Workshop, SP-696, ESA/ESTEC, Noordwijk, Netherlands.

Šprlák, M., Gerlach, C., Pettersen, B. R., 2012, Validation of GOCE global gravity field models using terrestrial gravity data in Norway. *Journal of Geodetic Science*, doi: 10.2478/v10156-011-0030-y.

Sømod, T., 1957, Gravimetric ties. Geodetiske arbeider, hefte 10. Norges geografiske oppmåling.

Tachikawa, T., Hato, M., Kaku, M., Iwasaki, A., 2011, The characteristic of ASTER GDEM version 2. In: IEEE International Geoscience and Remote Sensing Symposium (IGARSS), July 24–29, Vancouver, Canada, p. 3657–3660.

Tapley, B.D., Bettadpur, S., Watkins, M., and Reigber, C., 2004, The gravity recovery and climate experiment: Mission overview and early results. *Geophy. Res. Letters 31*, L09607, doi:10.1029/2004GL019920

Tenzer, R., and Klees, R., 2007, The choice of the spherical radial basis functions in local gravity field modeling. *Studia Geophysica et Geodaetica, 52(3)*, 287–304.

Torge, W., 1989, *Gravimetry. De Gruyter*, Berlin New-York.

Trovaag, O., and Jelstrup, G., 1950, Gravity Comparisons Olso-Teddington, Stockholm, Copenhagen. Den norske gradmålingskommisjon og norges geografiske oppmåling.

Tscherning, C.C., Arabelos, D.N., 2011, Gravity anomaly and gradient recovery from GOCE gradient data using LSC and comparison with known ground data. In: Proceedings of the 4th International GOCE User Workshop, SP-696, ESA/ESTEC, Noordwijk, The Netherlands.

Voigt, C., Rülke, A., Denker, H., Ihde, J., Liebsch, G., 2010, Validation of GOCE products by terrestrial sets in Germany. In: *Observation of the System Earth from Space, Geotechnologien*, No. 17, Potsdam, Germany, p. 106–111.

Voigt, C., Denker, H., 2011, Validation of GOCE gravity field models by astrogeodetic vertical deflections in Germany. In: Proceedings of the 4th International GOCE User Workshop, SP-696, ESA/ESTEC, Noordwijk, Netherlands.

Wenzel, H.G., 1998, Ultra high degree geopotential models GPM98A and GPM98B to degree 1800. In: Proceedings of Joint Meeting International Gravity Commission and International Geoid Commission, March 10–14, Budapest, Hungary, Rep 98:4, Finnish Geodetic Institute, Helsinki, p. 71–80.

Ågren, J., Svensson, R., 2007, Postglacial land uplift model and system definition for the new Swedish height system RH 2000. Reports in Geodesy and Geographical Information Systems, LMV-Rapport 2007:4, National Land Survey of Sweden, Gävle, Sweden, 124 p.